Improving functionality of Ti_6Al_4V by laser technology surfacing

S. V. SAVU, I. D. SAVU, G. C. BENGA, I. CIUPITU
University of Craiova, Drobeta Turnu Severin, Romania

Titanium is amazing material for wide applications due to its properties and its behaviour in specific conditions of exploitation. Against all these recommending characteristics, titanium has poor behaviour in conditions of friction. Wear processes are usually recorded during friction activity. Improving of the titanium's wear behaviour is possible by modification of the surface properties or by generating wear resistant layers using specific technologies. The paper presents experimental and theoretical analysis, performed in order to optimise the layer generation process. As base material, Ti_6Al_4V was used. Laser technology was used for the deposition of amorphous material. It has been considered two situations: modification of the surface by thermal cycle specific to simple laser beam melting and the generation by deposition of specific layer using laser technology and wear resistant adding materials. In the cases, optimization of the laser melting process was considered and hardness and structure of the new surfaces were analysed.

(Received April 11, 2016; accepted September 29, 2016)

Keywords: Titanium alloy, Wear resistance, Surfacing, Laser technology, Amorphous adding materials

1. Introduction

Titanium is high strength, low weight and outstanding corrosion resistance material. Due to those characteristics titanium met within the last 10 years wide and diversified range of applications which demand high levels of reliable performance in specific industries as prosthetics, aerospace, automotive, chemical plant, power generation, oil and gas extraction [1-3]. Some applications require more performances for titanium and new functionalities are expected to be offered to the titanium [2- 4]. From the required performances the wear resistance is the characteristic that brings higher reliability, economic and more durable systems and components, which in many situations have substantially exceeded performance and service life expectations. Scratching of the titanium is often met problem [1-4, 7]. If that is related to the aesthetics, simply removal of the scratches is possible by clean and polish with jewellery cloth. If the scratching is related to parts in contact of different mechanisms, then the influences brought by the scratches in the functionality of the parts are very important. The same situations are met in prosthetics, where any scratch of the surface could initiate irritations of the biomaterials in contact with the implant.

Generally, the titanium parts with surfaces in contact with other surfaces readily scratch under conditions of sliding contact or fretting [2]. Even if low loading is used during exploitation of the titanium, important seizure of surfaces can occur. That is mostly caused by adhesive wear in which microscopic asperities of the titanium surface come into contact with the asperities of the pair part as a result of relative sliding and they tend to weld together. The formed bond is possible to have tensile strength greater than the strength of the base metals in contact. Due to the relative movement of the parts, cracking of the bonds usually happens and the resulted particles will produce and accelerate an intensive wear process that occurs with titanium. The improvement of the functionality of the titanium is possible by developing specific alloys of titanium or by processing the core or the surface of the work-piece using different technologies, or both together [5,9,14-16]. The alloying of titanium produces two types of lattices: α which is hexagonal close packed and β which is body-centred cubic [3]. These structures are given by the alloying elements as follows: Al, O and Ga promote α structure and Mo, V, W, Ta, Cu, Mn, Fe, Ni, Co and H promote β structure. Because α structure gives good mechanical resistance, gives good weld-ability and good behaviour even in the cryogenic conditions, such structure is preferred. β structure improves the mechanical processing of the alloys and because of that the presence of a small quantity of β-phase within the mass of α-phase is often required by the users [3].

Ti_6Al_4V is α structure alloy with 4-6% weight elements that promote β-phase [8]. Vanadium is the main promoter of β-phase and after the reaction $\beta \rightarrow \alpha+\beta$ remains important quantity of β-phase [12,14]. The β-phase is lamellar one (Widmanstätten) if the alloy is high rate cool down from the α-phase. That means a significant increasing of the wear resistance, so solution to avoid scratching. In the same time such lamellar structure is fragile and the behaviour in shocks is poor. Better behaviour is met when the lamellar structure is only in the surface and that is possible by specific processing of the surface. Low penetration laser melting followed by high rate cooling is option as surfacing process. A second

option is to generate of special layer on the surface by using different deposition processes [4, 5, 9].

In the second option it should be discussed about residual stresses, distortion and hardness modifications..

2. Experimental details

Target-support of Ti_6Al_4V was subjected to modifications of the surface properties by two methods: a. simply melting and accelerated cooling and b. generations of high wear resistance layer by laser deposition. The base material presents mixture as granular structure: α+β phases. Inter-metallic compounds were revealed in uniform distribution. Table 1 presents the main properties of the base material as measured before the initiation of the experimental program.

Table 1. Mechanical characteristics of the base material

Base material	Tensile strength (N/mm^2)	Yield stress (N/mm^2)	Elongation (%)	Hardness HV1
Ti-Al-V	936	875	15	332,345,357

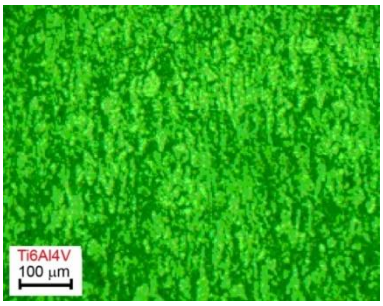

a.

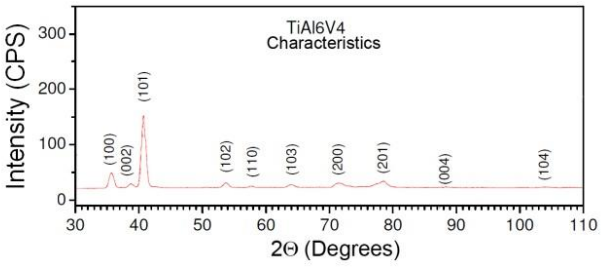

b.

Fig. 1. Characterization of the used Ti6Al4V

2.1. Laser technology to input energy into the surface

Laser technologies are based on focusing photons and transfer their energy on specific surface in order to modify the enthalpy of the target material [13]. The transfer of energy is limited by the reflection of the photons. Due to reflection, the intensity that is transmitted by the laser beam as thermal source, *I*, is lower than the intensity of the beam, I_{beam}, and the difference depends on the reflectivity of the target material, *R*.

$$I = I_{beam} \cdot (1 - R) \tag{1}$$

$$I_{beam} = \frac{I}{(1-R)} \tag{2}$$

The absorbance of the material is important when thermal field calculation is desired. Absorbance is generally defined by Beer-Lambert law as:

$$A = \ln\left(\frac{I_{beam}}{I_{mat}}\right) \tag{3}$$

$$I_{mat} = I_{beam} \cdot e^{\varepsilon \cdot l \cdot c} \tag{4}$$

where I_{mat} is the intensity of a virtual thermal source positioned inside the material and it is a model of the thermal front which is advancing to the core of the material due to I_{beam} that touches the surface, ε is the molar absorptivity (extinction coefficient) of the absorber and *c* is the molar concentration of absorbing species in the material, for a depth penetration *l*. Taking account that the laser beam is in motion by *v* travel speed (considering in x direction), the evolution of the thermal field it can be expressed as [10]:

$$\frac{\partial T}{\partial t} - v \cdot \frac{\partial T}{\partial x} = k \cdot \left(\frac{\partial^2 T}{\partial x^2} + \frac{\partial^2 T}{\partial y^2} + \frac{\partial^2 T}{\partial z^2}\right) + \frac{Q_{mat}(x,y,z,t)}{\rho_0 \cdot c_p} \tag{5}$$

where $\frac{\partial T}{\partial t}$ is the evolution of the temperature in time, $\frac{\partial T}{\partial x,y,z}$ is the evolution of the temperature in space, $Q_{mat}(x, y, z, t)$ is the thermal source inside the material (given by I_{mat}), ρ_0 is the density of the target material and c_p is the heat capacity of the target material. The thermal source inside the material is given by the intensity, I_{mat}:

$$Q_{mat}(x, y, z, t) = I_{mat} \cdot \alpha \tag{6}$$

where $\boldsymbol{\alpha}$ is the coefficient of absorption.

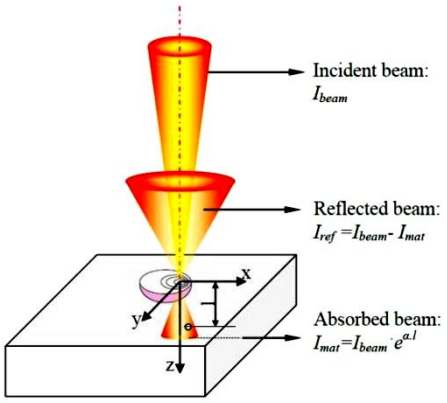

Fig. 2. Model of thermal transfer from beam to material

$$\frac{\partial T}{\partial t} - v \cdot \frac{\partial T}{\partial x} = k \cdot \left(\frac{\partial^2 T}{\partial x^2} + \frac{\partial^2 T}{\partial y^2} + \frac{\partial^2 T}{\partial z^2}\right) + \frac{I_{mat} \cdot \alpha}{\rho_0 \cdot c_p} \quad (7)$$

In which we will replace the expression of I_{mat} from equation 4:

$$\frac{\partial T}{\partial t} - v \cdot \frac{\partial T}{\partial x} = k \cdot \left(\frac{\partial^2 T}{\partial x^2} + \frac{\partial^2 T}{\partial y^2} + \frac{\partial^2 T}{\partial z^2}\right) + \frac{I_{beam} \cdot e^{\varepsilon \cdot l \cdot c} \cdot \alpha}{\rho_0 \cdot c_p} \quad (8)$$

Using the definition of absorbance, the multiplication $\varepsilon \cdot c$ is exactly the coefficient of absorption, α.

$$\frac{\partial T}{\partial t} - v \cdot \frac{\partial T}{\partial x} = k \cdot \left(\frac{\partial^2 T}{\partial x^2} + \frac{\partial^2 T}{\partial y^2} + \frac{\partial^2 T}{\partial z^2}\right) + \frac{I_{beam} \cdot e^{\alpha \cdot l \cdot \alpha}}{\rho_0 \cdot c_p} \quad (9)$$

Using the expression from equation 9 analysing of the temperature in a specific point, for $v \neq 0$ and concrete type of target material $(\varepsilon, l, c, \alpha, \rho_0, c_p)$, is possible. The values to build the thermal field will be calculated by applying integral to the equation 9. The solution of the integrated equation is:

$$T(x,y,z,t) - T_0 = \int_0^t 2 \cdot \frac{I_{beam} \cdot e^{\alpha \cdot l \cdot \alpha}}{\rho_0 \cdot c_p} \cdot [4 \cdot \pi \cdot k \cdot (t - t')]^{-3/2} \cdot e^{-\left\{\frac{[x + v \cdot (t-t')]^2 + y^2 + z^2}{4 \cdot k \cdot (t-t')}\right\}} dt' \quad (10)$$

To receive back a general solution, $t \to \infty$ is the condition to integrate and the equation 10 becomes:

$$T(x,y,z) - T_0 = 2 \cdot \frac{I_{beam} \cdot e^{\alpha \cdot l \cdot \alpha}}{\rho_0 \cdot c_p} \cdot \frac{1}{4 \cdot \pi \cdot k \cdot r} \cdot e^{-\frac{v \cdot (x+r)}{4 \cdot k}} \quad (11)$$

Considering a laser pulse of 2500 W and an average power of 100 W, for a frequency of pulses of 34 Hz the thermal field of the surface has the configuration from Fig. 3.

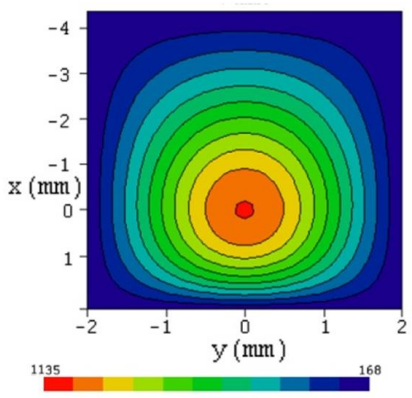

Fig. 3. Simulation of the thermal field model

Analysing the depth penetration of the heat, the evolution of the temperature on z axe is according to Fig. 4.

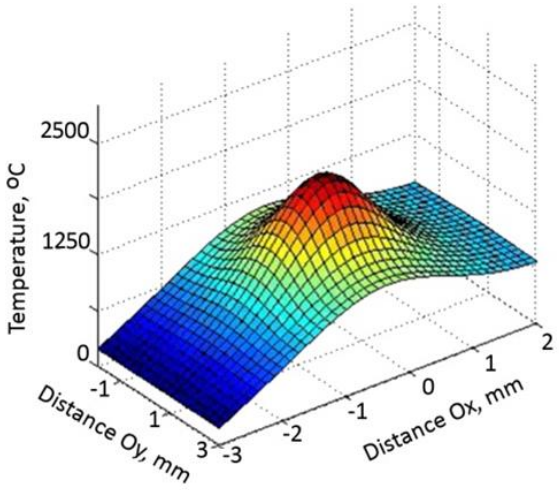

Fig. 4. Evolution of the heat to the core of the work-piece

The model helped to establish the heating parameters in order to control the penetration depth. It is important to maintain low penetration depth to have modification only at the level of a thin surface layer [9, 11].

2.1.1. Set up the equipment

The heating of the base material was done by pulsed laser process. For that, Nd:YAG laser (Trumpf HL 124P LCU) was used.

Table 2. Complete Factorial Exp. 2^3 + 2 C.P. (randomized, according to Statgraphics 5)

Test No.	Pulse power [W]	Pulse duration [ms]	Frequency [Hz]
1	3000	0.4	36.0
2	3200	0.5	32.0
3	3400	0.6	34.0
4	3600	0.7	34.0
5	3800	0.8	36.0
6	4000	0.4	4.0
7	4200	0.5	36.0
8	4400	0.6	32.0
9	4600	0.7	34.0
10	4800	0.8	36.0

The selected influence factors were (Table 2): pulse power [W], pulse duration [ms], pulse repetition rate [Hz], while the rest of the process parameters were kept on the same level: travel speed: 0,73 mm/s, spot diameter: 0.9 mm, pulse shape: rectangular, protection gas: Ar 99%. For the same frequency of the pulses (f = 34 hz) and for the same pulse time (t_p = 0.6 ms) the transmitted powers (pulse power and average power of the beam) are

presented in Fig. 5.

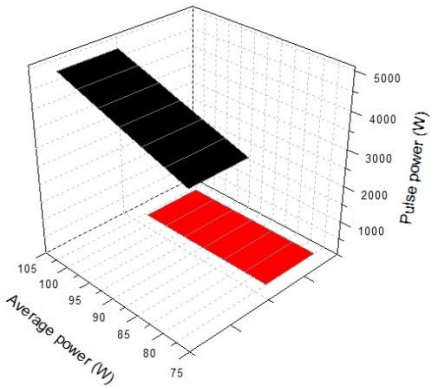

Fig. 5. Pulse and average power of the beam

2.1.2. Preparation of the base material

To avoid contamination of the base material, mechanical and chemical cleaning was necessary to be applied to the surface subjected to melting by laser [7, 9-11]. The applied mechanical cleaning consisted in brushing of the surface, cleaning designed to remove the solid particles of dust, oxides and grease. The chemical cleaning consisted in etching process, using a solution of 40% hydrofluoric acid and 40% nitric acid, followed by washing in plenty of water.

2.2. Melting process

The melting process was performed in controlled inert environment. Argon (99.98%) was used as inert shielding environment. The focal spot was positioned 2.1 mm under the surface of the work-piece, according to Fig. 6. The choice of the displacement of the focal point down to the core of the base material was based on the necessity to divide the energy of the laser beam on a surface instead punctual one. Such defocus reduces the local heating, so the local penetration. Preliminary experiments revealed that, lower than 2.0 mm distance from the surface to the core involves, higher concentration of the beam and the penetration is increasing. In the same time, higher than 2.5 mm distance means lower heating and no melting of the surface.

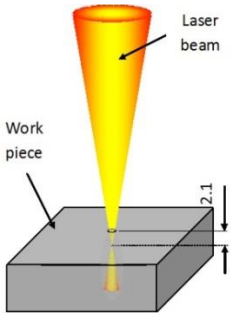

Fig. 6. Position of the focal point of the laser beam

As heating cycle two versions were designed and they are presented in Figs. 7a and 7b.

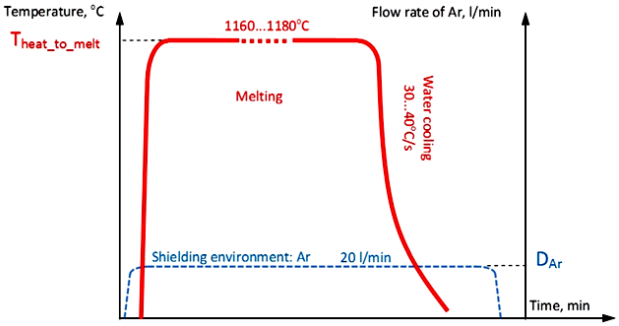

a. cycle 1

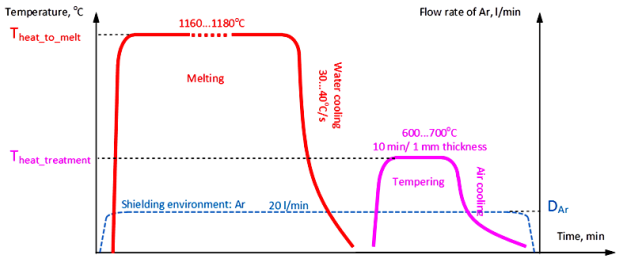

b. cycle 2

Fig. 7. Designed heating cycles

The first cycle was designed to offer a surface that is specific to high rate cooling. In that case it was expected to receive back Widmanstätten structure, brittle but with high wear resistance. The second cycle was design to reduce the brittleness of the surface in order to have good behaviour when shocks are met during exploitation.

The heating was applied in robotic system, travelling speed being constant, 1 m/min. After every heating cycle 15 min break were considered. Preliminary heating showed that 15 min is sufficient time to have appropriate cooling before the next heating cycle. Figs. 8 a. and b. show the resulted probes.

a. b.

Fig. 8. Melting of the work-piece a. performed with cycle 1, b. performed with cycle 2

3. Results and discussion

3.1. Characterization of the modified surface

Depending on the transmitted powers the depth of the penetration was recorded in the range 1.95…3.34 (Fig. 9). Lower penetration is better penetration for the deposition technology. After the melting, high rate cooling down (30…40°C/s) was applied. It was expected to receive back an increasing of the hardness necessary to offer better behaviour of the base material during working in sliding contact or fretting conditions.

Five HV1 hardness measurements have been applied for every set of parameters and the average is presented in Fig. 10. Lower than 20 HV1 difference between the 5 measurements of any regime has been obtained and that means that the complex process of melting and high rate cooling was uniformly applied on the entire surface.

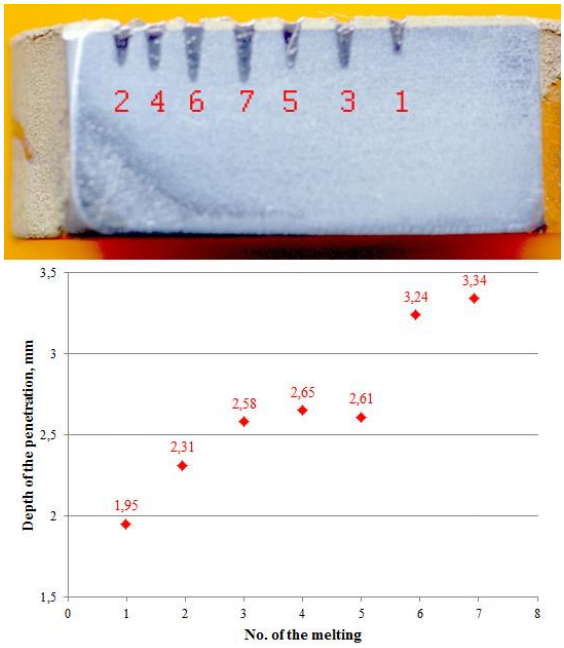

Fig. 9. Influence of the beam parameters on the penetration depth (cycle 1 as example)

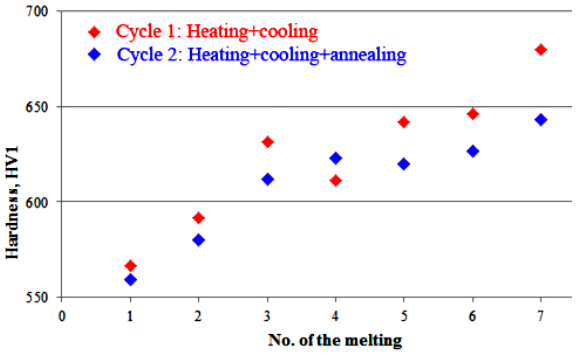

Fig. 10. Average hardness (5 HV1 testing points) of the molten and cooled down surface

Modifying the regimes in the way of the increasing the transferred power, higher values for the hardness were measured. Almost the same hardness has been obtained for average power in the range 85…95 W. For average powers lower than 85 W, the hardness of the heated material decreases with at least 100 HV1, so softer surface is maintained. Over 95 W average powers, hardness higher than 650HV1 was obtained and accentuated brittleness was manifested in the case of the cycle 1. When annealing treatment was applied after the heating cycle (cycle 2) softer surface was obtained, especially for high transferred power (>90 W).

Harmonising the penetration depth with the hardness, it can be considered that the optimum transferred powers are in the range of 80…90 W for cycle 1 and in the range of 80…105 W for cycle 2. Annealing modified the structure of the surface reducing the Widmanstätten volume (Fig. 11b) comparing to the structure obtained with cycle 1 (Fig. 11a).

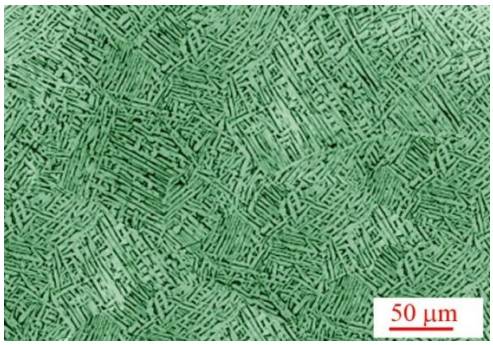

a. Widmanstättenβ structure – obtained from high rate cooling of α in cycle1 heating

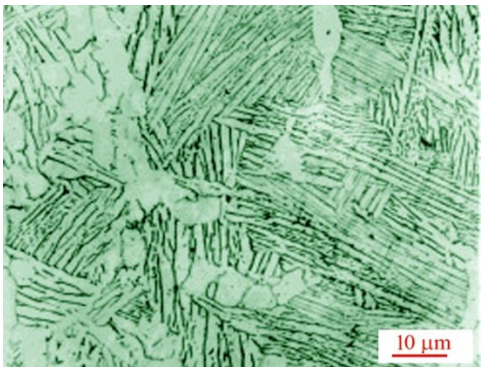

b. α structure and Widmanstätten β structure obtained from annealing of Widmanstätten β in cycle 2

Fig. 11. Structure of the surface after the heating process

The modification of the structure after the heating cycles could be considered as being influenced by a decreasing of the thermal conductivity which was revealed, as well.

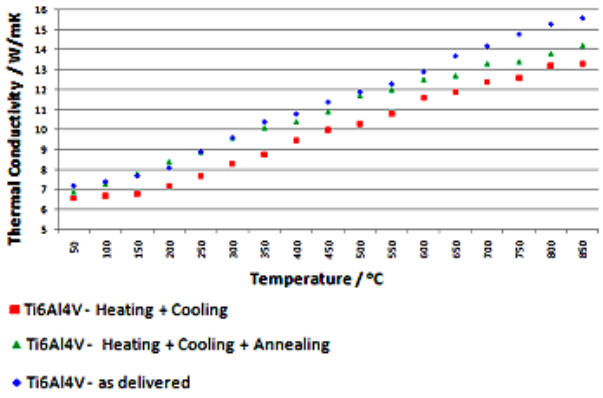

Fig. 12. Decreased thermal conductivity after the heating cycle

3.2. Layer generation by thermal spraying deposition and laser formation of the layer

3.2.1. Conditions for deposition process

Layer generation is the second method of conditioning surface of Ti_6Al_4V that was used within the experimental programme. The method consisted in complex process: deposition of molten metal with high wear resistance by thermal arc-spraying and the re-melting of the deposited layer by laser heating cycle. The wear resistant metal deposited on the surface was obtained by spraying wire with the chemical composition presented in Table 3. As thermal spraying process, classic arc spraying using 2 wires was used for the deposition process.

Table 3. Chemical composition of the sprayed wire, %

Cr	Ni	Mn	Mo	Si	C	Fe
17.00	12.00	2.00	2.50	1.00	0.08	rest

Thermal spraying deposition was manual but, because of low surface of the work-piece, it was uniform. Fig. 13 shows the probe of Ti_6Al_4V after the thermal spraying process.

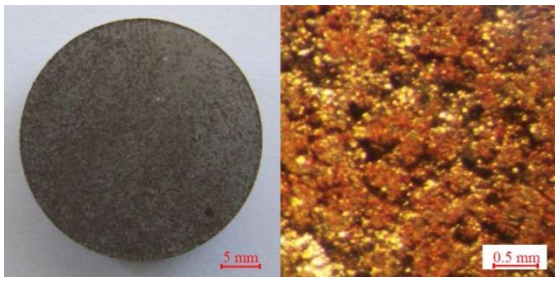

Fig. 13. Thermal sprayed probe

Nine melting passes were necessary to cover the surface required for analysis. Fig. 14 presents the work-piece after the layer generation process.

Fig. 14. Conditioned surface by successive melting strings

3.2.2. Characterization of the deposited layer

The width of the laser melting was in the range of 1.5…2.5 mm. After every melting pass 10 min break for natural cooling was applied. The surfaces of the deposition strings and the areas between the strings were clean and no cracks were detected on the surface of the deposited layer. Metallographic examination of the molten area of the base material revealed dendrite structure, specific to casting of mixing of titanium and foreign molten powders. Fig. 15 presents the α+β structure of the base material and contaminations with different alloys and inter-metallic compounds.

Hardness test was performed to every string (3 tests per string). Values in the range of 660…720 HV1 were obtained. The brittleness of the surface was tested by technological tests with shock application and it was considered low. The adherence of the deposited layer was considered high because of the laser melting process. XRD analysis (Fig. 16) revealed increasing of the intensities and higher volume of β structure. That means better behaviour in machining processes, which are necessary to offer smooth surfaces for exploitation.

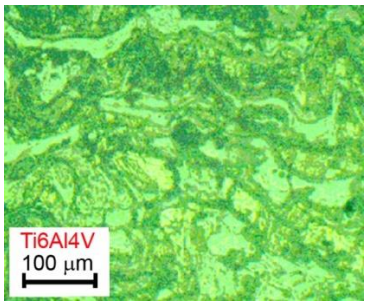

Fig. 15. Structure of the surface formed by mixing the molten base material with the molten powder

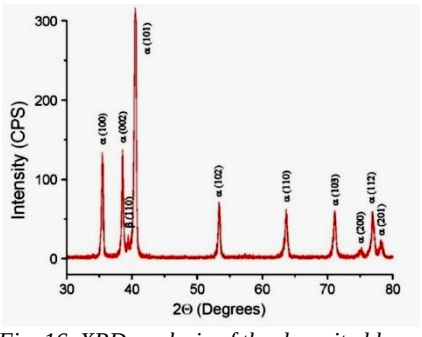

Fig. 16. XRD analysis of the deposited layer

The oxidation of the base material during the heating process affects the functionality of the surface. Oxidation kinetics [16] of the base material were performed by using thermo-gravimetry (TG) analysis between 200 and 700/°C for 48 hours (Netzsch Jupiter STA 409CD).

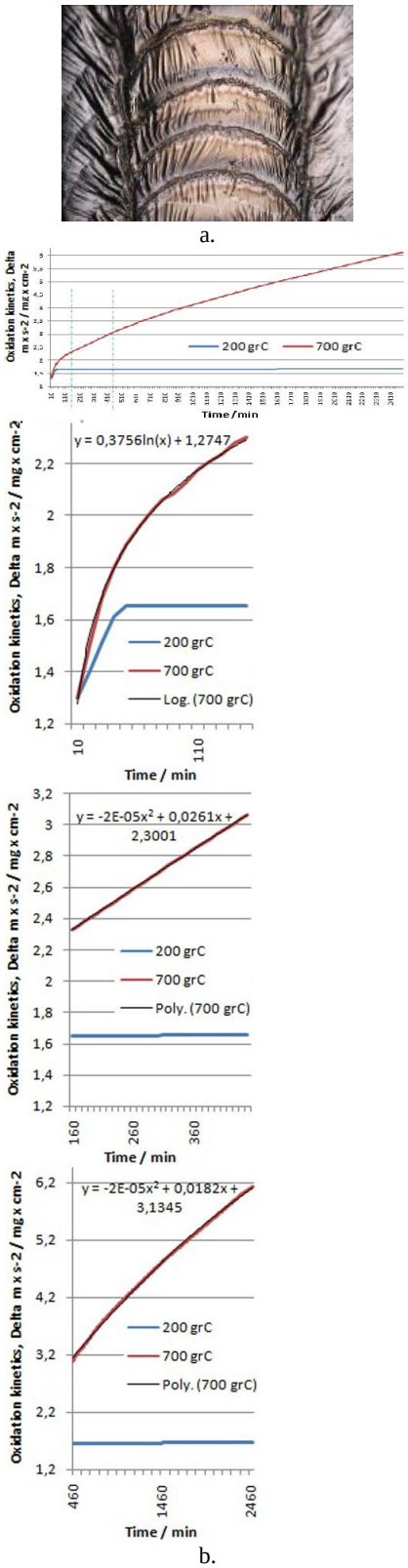

a.

b.

a. oxidized surface, b. oxiding kinetics
Fig. 17. Oxiding process

According to Fig. 17b the slowest oxidation was registered between 160 and 460 min and the values specific to those heating speeds were below half of the maximum speed which has been recorded after 2500 min.

3.3 Friction coefficient determination

Determinations of the friction coefficient were performed using pin-on-disk tribometer for friction and wear characterization according to ASTM G99-04 (Fig. 18a).

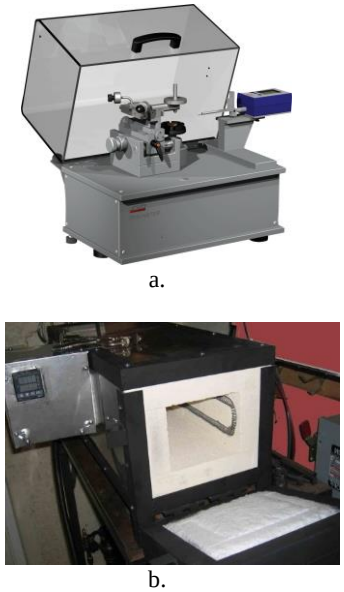

a.

b.

Fig. 18. Pin-on-disk tribometer and oven used in preparation and testing the specimens

For the tests all the surfaces subjected to test were polished in the same manner. Before test, each specimen was cleaned in acetone in ultrasonic bath for 15 min. After cleaning the specimens were dried in heat treatment oven (Fig. 18b) at 90 ^{o}C for 30 min. The cooling was natural, down to the room temperature. Force of 2 N and sliding speed of 0.1 m/s were considered for the tests. The total sliding distance was 420 m for each test with a wear track diameter of 30 mm. Room temperatures (controlled 22±1 ^{o}C) and max 75 % humidity were the environmental conditions of the tests. All the tests were applied for 70 min. 20 tests of determination of friction coefficient were performed – 5 tests for each of: for the base material, for the laser heating modification of the surface applying cycle 1, for the laser heating modification of the surface applying cycle 2 and for the deposited layer by thermal spraying and laser melting. The disk specific wear was evaluated using profilometer. The profiles, taken in 2 positions, were integrated using the profilometer software to obtain the wear scar area, then averaged and multiplied for the track length.

Figs. 19 a, b, c and d show the evolution of the friction coefficient for the 4 tests.

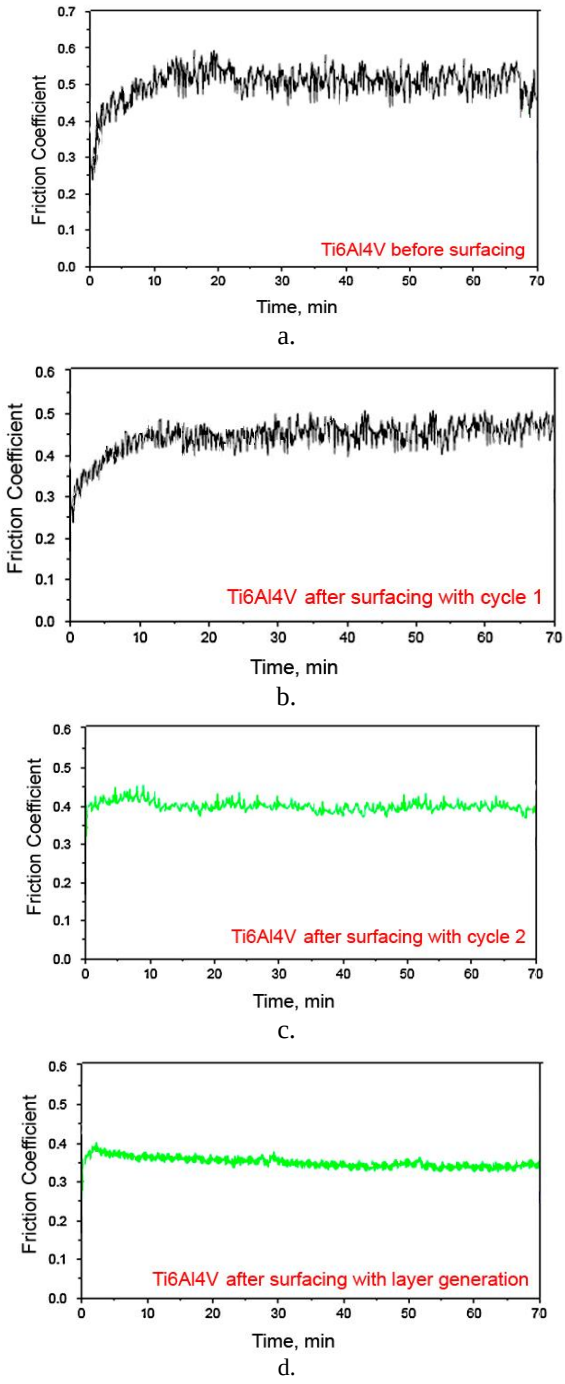

Fig. 19. Friction coefficient after the 4 tests according to ASTM G99-04

Figs. 19 a and b show important dispersion of the values even if the preparation of the surface was similar to the probes presented in Fig. 19 c and d (painted in green). That means that the dispersion of the hardness on the surface is important and that is considered unacceptable for the application mentioned above. The evolutions from Figs. 19 c and d are considered acceptable as dispersion of the values. Comparing to the values recorded for the base material Ti_6Al_4V it can be observed a decreasing of the friction coefficient with about 20%, from 0.5 to 0.4.the optimal result was obtained for the layer deposited by thermal spraying followed by laser re-melting of the particles.

As general results of the analysis, the following are to be considered.

Laser heating followed by high rate cooling was applied in two versions: a. heating to melting and high rate (30…40^{o}C/s) cooling and b. heating to melting and high rate (30…40^{o}C/s) cooling followed by annealing treatment in order to reduce the brittleness by reducing the volume of the Widmanstätten structure volume. In the both cases the depth of the penetration was limited to about 3mm by controlling the heat input. It was considered, from previous expertise, that higher than 3 mm penetration produces stress and cracking process could occur. The control of the heat input depends on the laser beam intensity, and model was proposed in order to help us to choose the laser beam parameters. The model is based on two distinct things: the absorbance of the base material and the heat conduction inside the base material. Putting together the two aspects it was possible to build a model which links the thermal field with the laser parameters. Controlling the parameters according to the model it was possible to control the penetration and the hardness of the surface. Every version of the process' cycle returned specific structure. Both of them presented Widmanstätten structure, but the treatment of annealing from the cycle 2 reduced the brittleness of the surface. The treatment of annealing consisted in the reheating from the room temperature up to 600…700^{o}C with a maintaining of 10 min / 1 mm of thickness. The heating was followed by air cooling. The entire process of heating plus cooling and annealing (cycle 2) was performed in controlled environment. Argon was used as environment to avoid the oxidation of the base material, 20 l/min being the flow rate of argon as shielding gas. The hardness of the surface increased with the input power and the optimal values (600…650 HV1) were obtained for an average input power of 85…95 W. The obtained values for the both cases were 70…80% higher than the values measured for the base material and that means a significant increasing of the resistance during wear processes. The special surface layer generation, by thermal spraying, and the re-melting of the powder, by using laser heating, were different technological solutions considered for the solving of the Ti_6Al_4V problem. The active surface was built on the base material, the characteristics of the surface being the characteristics of the deposited layer. The deposited metal was provided by melting wire dedicated to wear resistance purposes. The thickness of the wire was 1.6 mm and the chemical composition presented high contents of chromium (17%) and nickel (12%), as well as manganese and molybdenum, both higher than 2% content. The content of chromium together with manganese and the molybdenum increased the hardness of the deposited material. In the same time, the content of chromium together with the content of nickel improved the corrosion resistance (specific to austenitic stainless steel). Not verified yet, but expected, an increasing of the behaviour at temperatures higher than 400^{o}C is also a characteristic of the layer. The deposited layer was examined under

microscope and specific structure of Ti_6Al_4V contaminated with alloys, carbides of chromium or inter-metallic compounds. The morphology of the layer was specific to the thermal sprayed layers, where full molten and partial molten particles are fixed each other. Applying Vickers hardness test, it have been revealed values in the range of 660...720 HV1. Comparing to the values measured for the conditioning of the existent surface (without building special layer) it can be observed a difference of about 100 HV1 (15...20% bigger than in the case of the special deposited layer). If 70...80% increasing of hardness has been measured for the conditioning of the surface, about 90% increasing has been recorded for the deposited layer. Better wear resistance will be provided by the special deposited layer. From any applied processing method, selected probes were used for tribometric analysis. Friction coefficient has been measured using pin-on-disk method, after polishing of the tested surfaces. For the specimen extracted from the base material, important dispersion of the values was revealed (Fig. 17 a). That means those different torques were sensed by the testing equipment. Similar situation has been revealed when the cycle 1 of processing was applied. Different to those both cases were the results obtained for cycle 2 of processing and for the generation of special surface by spraying and laser re-melting. Here, the dispersion of the recorded data regarding the friction coefficient was sensitively lower. In all 20 tests the values of the friction coefficient was in the range 0.35 ... 0.45 (cycle 1: average value around 0.42 ... 0.45, cycle 2: average value around 0.39 ... 0.41 and for the generated layer the average value was around 0.35 ... 0.37).

4. Conclusions

Titanium returns poor behaviour in wear activity. Scratching of any titanium alloy affects the exploitation of the technical components, especially the components for medical purposes, as prosthetics. Improving the wear resistance is possible by conditioning the active surface of the components. By conditioning we mean modification of the characteristics of the surface by laser heating and high rate cooling, or by generating special layers using specific deposition processes.

As general conclusion the improving of the Ti_6Al_4V surface wear resistance is possible by all applied methods. The cheapest method is the simply heat and cool down, according to cycle 1, but the improvement of the functionality of the surface is lower than necessary. The generation of special wear resistant layer on the surface of the Ti_6Al_4V was the solution with the optimal technical results, but not the most economic.

The heating produced a decreasing of the thermal conductivity and that could partially explain the modification of the structure. In the same time, due to the heating process, oxidizing of the surface occurred and the kinetics of the oxidizing process can be controlled by controlling the heating time.

References

[1] L. L. Badita, G. Gheorghe, J. Optoelectron. Adv. M. **16**(7-8), 945 (2014).
[2] W. Xu, et al., Applied Surface Science **259**, 616 (2012).
[3] Z. Wang, et al., Applied Surface Science **257**(23), 10267 (2011).
[4] M. Stoicanescu, C. Pitulice, I. Giacomelli, J. Optoelectron. Adv. M. **17**(9-10), 1411 (2015).
[5] R. M. Mahamood, E. T. Akinlabi, J. Optoelectron. Adv. M. **17**(9-10), 1349 (2015).
[6] H. Bros, M. -L. Michel, R. Castanet, Journal of thermal analysis, **41**(1), 7 (1994).
[7] M. E. Khosroshahi, M. Mahmoodi, J. Tavakoli, Applied Surface Science **253**(21), 8772 (2007).
[8] G. P. Dinda, et. al, The Minerals, Metals & Materials Society and ASM International 2008.
[9] M. Lassri, H. Ouahmane, H. Lassri, J. Optoelectron. Adv. M. **15**(11-12), 1295 (2013).
[10] O. Turcan, O. Dontu, J. L. Ocana Moreno, I. Voiculescu, D. Savastru, I. M. Vasile, J. Optoelectron. Adv. M. **16** (1-2), 20 (2014).
[11] J. L. Ocaña, C. Molpeceres, J. J. Garcia-Ballesteros, S. Lauzurica, D. Iordachescu, J. Optoelectron. Adv. M. **13**(8), 976 (2011).
[12] S. Kumar, et. al., Materials Chemistry and Physics **119**(1-2), 337 (2010).
[13] D. Iordachescu, M. Blasco, R. Lopez, A. Cuesta, M. Iordachescu, J. L. Ocaña, J. Optoelectron. Adv. M. **13**(8), 981 (2011).
[14] I. Halevy, et. al, Journal of Physics: Conference Series **215**, 012013 (2010).
[15] A. Przepiera, M. Jablonski, J. of Therm. Anal. and Calorimetry, **74**(2), 631 (2003).
[16] E. Kaschnitz, P. Reiter, J. of Therm. Anal. and Calorimetry, **64**(1), 351 (2001).

*Corresponding author: sorin.savu@yahoo.com